Comparing the Chloride Resistances of Reinforcing Bars

Evaluating new, economical metallic reinforcement for its ability to withstand high salt concentrations

BY GERARDO G. CLEMEÑA AND YASH PAUL VIRMANI

Prompted by increasing construction costs and lack of funding for maintenance and new construction, many state transportation agencies now specify a design life of 75 and 100 years for minor and major concrete bridges, respectively, without major repairs. Chloride-induced corrosion of reinforcing bars, however, has been a primary cause of premature deterioration of many concrete bridges. Achieving these service-life goals requires either improvement of current epoxy-coated carbon steel bars (ECR) or development of new bars that are more corrosion resistant and reasonably affordable.

Because of the need for an economical, corrosion-resistant bar, several new bars have recently been introduced to the industry: 1) a "positive-machined" stainless steel bar (R304); 2) a stainless steel-clad carbon steel bar (316L); 3) a "microcomposite" steel bar; 4) a "lean" duplex stainless steel bar (2101 LDX); and 5) a carbon steel bar coated with a 2 mil (0.05 mm) layer of arc-sprayed zinc and an epoxy coating (Zn/EC). Because at least one of these bars might contribute to significantly increasing the service life of future concrete bridges in a cost-efficient manner, we compared their resistances to corrosion in heavily salted concrete blocks with that of conventional carbon steel (CS) bars and austenitic stainless steel bars (316 LN). This article discusses the results of the study obtained thus far. Reference 1 reported a similar comparison of the clad bars with the same stainless steel bars in simulated concrete pore solutions.

STAINLESS = CORROSIONLESS

Bars made of certain austenitic stainless steels, which are intrinsically corrosion resistant, are able to withstand high concentrations of chlorides in concrete, as indicated in several investigations conducted since 1985.[2-5] Concrete bridges built with any of these bars will last a long time, likely much longer than those built with ECRs. The average cost of in-place stainless steel bars, however, is prohibitively high—more than four times that of ECRs.

The R304 bars used in this study were made in the U.K. by welding stainless steel wires (grade 304 per ASTM A 314) onto round stainless steel rods (grade 304 per ASTM A 314) to form the ribs. By producing the bars in this manner, the UK company predicted that it could market the bars at half the cost of conventional stainless steel bars.

The production of the stainless steel-clad bars involved packing 316L grade (per ASTM A 314) stainless steel pipes with fine granules of CS. These compacted, composite pipes were then heated in a furnace with a reducing environment up to 1250 °C (2280 °F) and hot rolled into 316L-clad bars of appropriate sizes. The stainless steel cladding provides extremely durable, yet economical, protection to the CS core.

The 2101 LDX lean, duplex stainless steel is relatively less costly than typical stainless steel with nominal chromium and nickel contents of 21 and 1.5%, respectively. The microcomposite steel alloy contains approximately 9% chromium. In the experimental Zn/EC bars, the Zn layer provides galvanic protection to the steel wherever there is damage to the epoxy coating.

TABLE 1:
TEST CONCRETE BLOCKS

Bar material	Bar combination		No. of blocks	Block designation
	Top bars	Bottom bars		
Carbon steel	Straight carbon steel	Straight carbon steel	4	CS/CS
	Bent carbon steel	Straight carbon steel	8	Bent CS/CS (1)*
	Bent carbon steel	Straight carbon steel	4	Bent CS/CS (2)*
316LN	Straight 316LN	Straight 316LN	4	316LN/316LN
	Straight 316LN	Straight carbon steel	4	316LN/CS
	Bent 316LN	Straight carbon steel	8	Bent 316LN/CS
R304	Straight R-304	Straight R-304	4	R304/R304
	Straight R-304	Straight carbon steel	4	R304/CS
	Bent R-304	Straight carbon steel	8	Bent R304/CS
316L-clad	Straight clad bar	Straight clad bar	4	CB/CB
	Straight clad bar (w/holes)	Straight clad bar	4	CB (w/holes)/CB
	Straight clad bar	Straight carbon steel	4	CB/CS
	Bent clad bar	Straight carbon steel	8	Bent CB/CS
	Bent clad bar (w/cut)	Straight clad bar	4	CB (w/cut)/CB
Microcomposite	Bent microcomposite	Straight microcomposite	4	MC/MC
2101 LDX	Bent 2101 LDX	Straight 2101 LDX	4	2101/2101
Zn/EC	Bent Zn/EC-1	Straight Zn/EC-3	4	Zn/EC-1
	Bent Zn/EC-2	Straight Zn/EC-3	4	Zn/EC-2
	Bent Zn/EC-3	Straight Zn/EC-3	4	Zn/EC-3

* Denotes either Series-1 or -2 concrete blocks.

REINFORCEMENT TESTED

The two benchmark bars represent different ends of the corrosion-resistance spectrum—with poor corrosion resistance represented by the CS bar and excellent corrosion resistance represented by the 316LN bar. We tested both straight and U-bent bars. The surface conditions of all bars were not modified from those provided by their suppliers: the 316LN, R304, and clad bars were all pickled, while the 2101 LDX and microcomposite steel bars were not. Although the other bars had a nominal diameter of 16 mm (0.62 in.), the microcomposite steel and the 316L-clad bars had nominal diameters of 13 and 19 mm (0.50 and 0.75 in.), respectively.

The mean thickness of the stainless steel cladding on these bars was 1.08 mm (42 mil), with a standard deviation of 0.23 mm (9 mil). The minimum and maximum thickness was 0.44 and 1.43 mm (17 and 56 mil), respectively. To assess the effects of possible defects in the stainless steel cladding on the CS core, three 0.5-mm-wide (0.020 in.) holes were intentionally drilled through the cladding in several 316L-clad bars. In several other 316L-clad bars, a 25-mm-long (1.0 in.) and 1-mm-wide (0.04 in.) cut was made to expose the CS core before they were embedded in concrete.

To determine how the Zn/EC bars might behave if there was damage to the composite coating system, an approximately 25 mm (1.0 in.) cut was intentionally introduced through the Zn and the epoxy coating to expose the CS on some of these bars, which were designated as Zn/EC-1. We estimate the widths of the cuts to be 0.025 to 0.076 mm (1 to 3 mil). On another group of Zn/EC bars, designated Zn/EC-2, the 25 mm (1.0 in.) cut was intentionally introduced on the epoxy coating only. On the remaining Zn/EC bars, designated as Zn/EC-3, no cuts were made.

CONCRETE BLOCKS AND ACCELERATED SALT EXPOSURE

Several sets of concrete blocks (Fig. 1) were constructed with the different bars embedded in the various combinations listed in Table 1. To assess the possible consequences of using one type of bar at the top mat and another at the bottom mat of a concrete bridge deck (to reduce materials cost) some blocks were fabricated with 316LN, R304, or 316L-clad bars at the top and CS bars at the bottom. The concrete blocks for the 2101 LDX, the microcomposite, and the Zn/EC bars were constructed (using the same mixture proportions) approximately 1 year after the

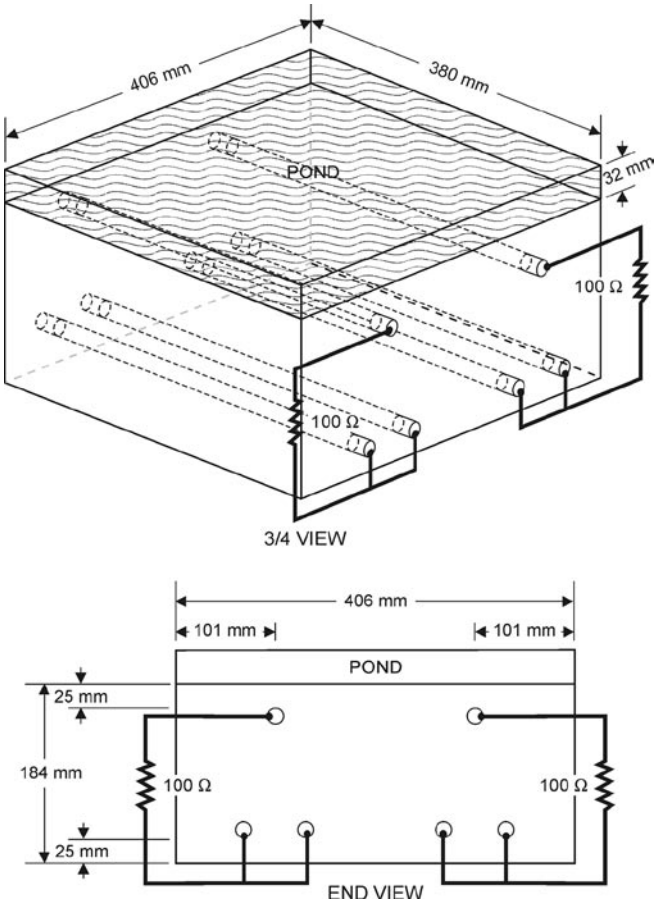

Fig. 1: Concrete test blocks contained either straight or bent bars at the top, while all bottom bars were straight

blocks for the 316L-clad and the R304 bars. Concrete blocks with CS bars (to serve as controls) were also constructed at the same time.

A few days after the test blocks were fabricated (using the mixture proportions given in Table 2) the forms were removed and wooden dams were built on top of the blocks. Then, all the concrete blocks were covered with sheets of heavy plastic and allowed to cure outdoors for approximately 4 weeks before the sides of each block were coated with a rapid-setting epoxy. Following this, all the test blocks were subjected to weekly cycles of ponding with a saturated solution of NaCl for 3 days and drying for 4 days. To minimize differences in outdoor exposure conditions, and to compare the results from the first and the second series of concrete blocks, the exposure of the second series to the salt solution began on September 17, 2001, nearly 1 year after the beginning of exposure of the first series (started on September 8, 2000).

MEASUREMENTS MADE

We measured the macrocell current flowing between bars in the top and bottom of each concrete block

TABLE 2:
MIXTURE PROPORTIONS FOR THE CONCRETE TEST BLOCKS

Water-cement ratio (*w*/*c*)	0.50
Cement, kg/m^3	390
Coarse aggregates, kg/m^3	1059
Fine aggregates, kg/m^3	828

Note: 1 kg/m^3 = 1.685 lb/yd^3

weekly to define the initiation of corrosion on the different bars. This measurement was made using the voltage-drop method. In this manner, a negative voltage drop corresponds to a positive macrocell (galvanic) current (the top bars would be anodic compared to the bottom bars). Finally, the macrocell currents for all the top bars in the same subset of concrete blocks were averaged to yield the subset mean macrocell current for each weekly measurement.

The open-circuit potential of each top bar was also measured with a $Cu/CuSO_4$ electrode (CSE). Before each measurement, the electrode was placed directly over the center of the top bar, which was disconnected from its corresponding bottom bars.

To allow for estimation of the amount of chloride ions that penetrated the concrete blocks after various salt exposure cycles, we determined the concentrations of the total (acid-soluble) chloride in 16 concrete blocks, at depths ranging from 13 to 51 mm (1/2 to 2 in.) and exposure times ranging from 114 to 661 days, according to ASTM C 1152.

Macrocell currents

In a concrete bridge deck exposed to deicing salts, the top-mat reinforcing bars are typically the first ones to be exposed to moisture and chloride ions. This gives rise to concentration gradients of these substances and, therefore, electrochemical macrocells in the concrete. Once a macrocell is created in the concrete, the top bars become more anodic than the bottom ones and a current flows between them. It is believed that these macrocells are the major driving force of reinforcement corrosion and the resulting delamination of the surrounding concrete. The concrete blocks in this study, and the manner with which they were exposed to salt, simulated this situation in concrete bridge decks.

As basis for comparison, Fig. 2 shows the weekly macrocell currents of the two subsets of concrete blocks—one was part of the Series 1 and the other of the Series 2 blocks—that were reinforced with bent CS bars at the top and straight CS bars at the bottom (Bent CS/CS (1) and (2)) as these blocks were being subjected to outdoor weekly cycles of salt ponding and drying. As Fig. 2 shows, the top bent CS bars in both series of concrete blocks were initially passive, with mean macrocell

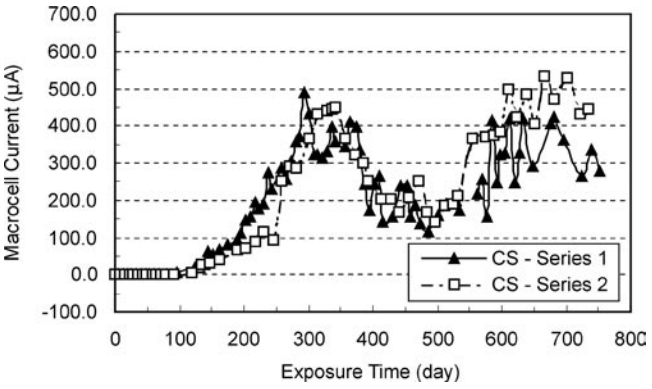

Fig. 2: Macrocell currents of the two sets of concrete blocks with bent CS bars at the top and straight CS bars at the bottom of each block

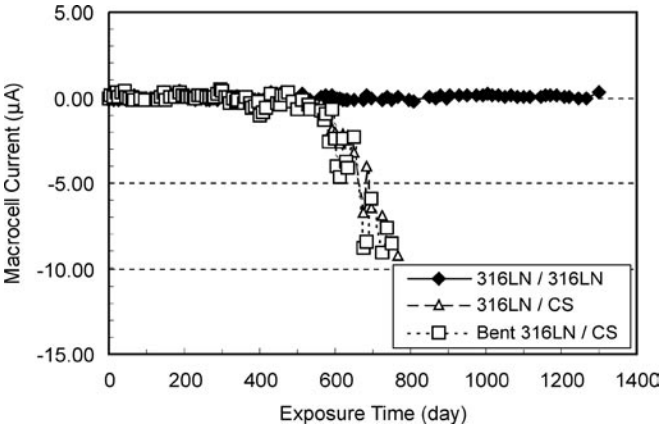

Fig. 3: Macrocell current of the concrete blocks with 316LN bars in various combinations described in Table 1

currents of about 0.1 µA. This level of macrocell current can be considered insignificant because the accuracy of the measurement is ± 0.2 µA. Then, beginning between days 90 and 95, the macrocell currents of both sets of concrete blocks began to exhibit rapid increases. This indicates that sufficient chloride ions had reached the top CS bars causing them to become anodic with respect to the CS bottom bars. During the 752 days of outdoor exposure of the concrete blocks with Bent CS/CS (1), the mean and the maximum macrocell currents observed were 208.5 and 490.7 µA, respectively. For the concrete blocks with Bent CS/CS (2), the mean and the maximum macrocell currents observed were 217.6 and 534.9 µA, respectively, during 735 days of exposure. (Table 3 lists the mean and maximum macrocell currents observed for these two sets of test blocks and all other sets of test blocks.) With differences of only 9 and 4% for the mean and the maximum macrocell currents, respectively, between these two series of concrete blocks, the results presented in Fig. 2 are in good agreement.

Although not presented, the results of the concrete blocks with straight CS bars at the top (CS/CS) were similar to the results for the bent CS bars (Bent CS/CS (1)). Most important, the macrocell current of these blocks (CS/CS) did not become significant until after 90 days of weekly salt exposure. Their mean and maximum macrocell currents, however, were lower—only 57.2 and 229.5 µA, respectively. Such difference in the apparent corrosion activities of straight and bent CS bars, although not consistently, has been observed before.

Macrocell currents in the two sets of test blocks (Bent CS/CS (1) and (2)) were concurrent with changes in the outdoor exposure conditions (temperature and rainfall) with the seasons (Fig. 2). In general, peaks and valleys in the currents for the two sets of test

TABLE 3:
MACROCELL CURRENTS OBSERVED ON VARIOUS GROUPS OF TEST CONCRETE BLOCKS

Test blocks	Macrocell current, µA		Total exposure time, day
	Mean	Maximum	
CS/CS	57.2 ± 0.2	229.5 ± 0.2	865
Bent CS/CS (1)	208.5	490.7	752
Bent CS/CS (2)	217.6	534.9	735
316LN/316LN	0.0	0.4	1299
316LN/CS	−0.9	−9.2	752
Bent 316LN/CS	−1.0	−9.0	752
R304/R304	0.0	0.3	1299
R304/CS	−0.5	−4.7	752
Bent R304/CS	−0.1	−2.5	752
CB/CB	0.0	0.2	1299
CB (w/holes)/CB	0.0	0.3	1299
Bent CB (w/cut)/CB	0.9	10.5	899
CB/CS	−1.4	−9.4	752
Bent CB/CS	−4.3	−26.5	752
2101/ 2101	89.0	209.8	805
MC / MC	77.2	231.2	805
Zn/EC-1 / Zn/EC-3	0.1	0.8	899
Zn/EC-2 / Zn/EC-3	0.0	0.3	899
Zn/EC-3 / Zn/EC-3	0.0	0.3	899

Note: The sign indicates the direction of current flow between the top and the bottom mats.

Fig. 4: Side view of a concrete block with 316LN bars at the top and CS bars at the bottom

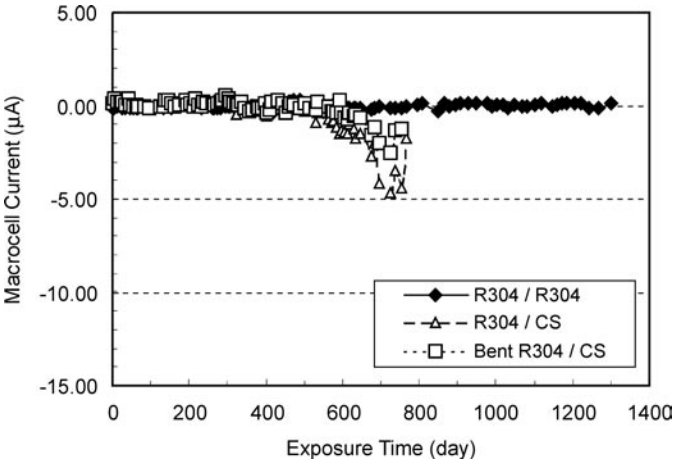

Fig. 5: Macrocell current of the concrete blocks with R304 bars in various combinations

blocks corresponded to warmer spring and summer days and colder winter days, respectively.

For those blocks with 316LN bars in the top and bottom (316LN/316LN), weekly macrocell currents after 1299 days (or 186 weekly cycles) of salt exposure were insignificant, averaging 0.0 µA at a standard deviation of ± 0.2 µA, which indicates that the bars were passive (Table 3). In addition, Fig. 3 shows that after about 400 days, the concrete blocks with 316LN bars at the top and CS bars at the bottom (316LN/CS and Bent 316LN/CS) began to exhibit negative macrocell currents. This indicated that sufficient chloride ions had reached the CS bars so that they became more anodic than the top 316LN bars and were corroding. As indicated in Table 3, the macrocell currents for these two subsets of blocks reached –9.0 and –9.2 µA before we stopped taking measurements (at approximately 752 days) due to cracking of some of the blocks near the bottom CS bars (see Fig. 4).

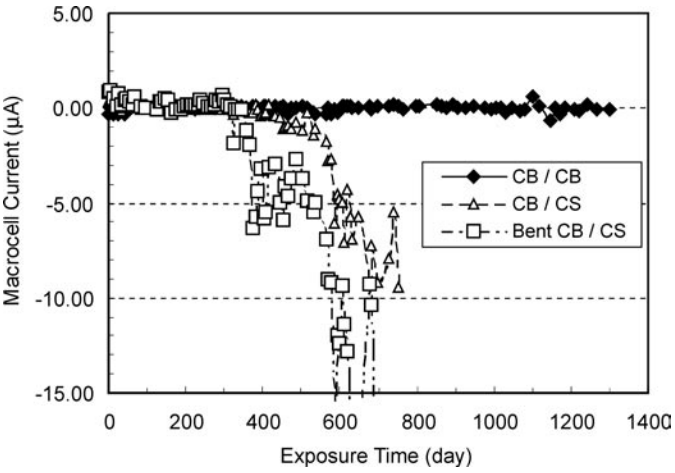

Fig. 6: Macrocell current of the concrete blocks with 316L-clad bars in various combinations

Graphs for the R304 and 316L-clad bars (Fig. 5 and 6, respectively) show similar results to that of Fig. 3 for the 316LN bars. All of these graphs share two common characteristics. First, the concrete blocks containing either 316LN, R304, or 316L-clad bars in both mats, even after 1299 days of the salt exposure regime, lack any significant macrocell current. This implies that the R304 bars, which are basically a solid 304 stainless steel, and the 316L-clad bars had, so far, exhibited the same good resistance to attack by chloride ions in concrete as the solid 316LN bars had. Second, negative macrocell currents (after 350 to 450 days) appeared in the blocks where CS bars were used in the bottom mat. Noteworthy is the smaller negative macrocell currents in the blocks with CS bars and R304 bars, compared to those with the 316LN and the 316L-clad bars, as shown in Fig. 3, 5, and 6. Perhaps this is a reflection that R304 is relatively less noble than 316L and 316LN.

To prove that such negative macrocell currents were caused by the bottom CS bars corroding before the more corrosion-resistant bars at the top, four sets of those concrete blocks (showing negative currents) were flipped upside down after about 270 days. We measured the potentials and corrosion rates of the bottom CS bars, the latter using the linear polarization method. The potentials of some of the bars were between –352 and –506 mV and the corrosion rates were as high as 1.8 to 37.3 µA/cm^2. Based on commonly accepted interpretation[6] that a measured corrosion rate of >1.0 µA/cm^2 for conventional steel bars indicates presence of active corrosion, there is little doubt that these bottom CS bars were corroding.

We did not observe macrocell currents in the concrete blocks with either the unpickled 2101 LDX or the unpickled microcomposite steel bars until after 147 or 245 days of exposure, respectively. Interestingly, the effect of seasonal variations in outdoor conditions on the macrocell currents of the CS bars is also evident in these two bar types.

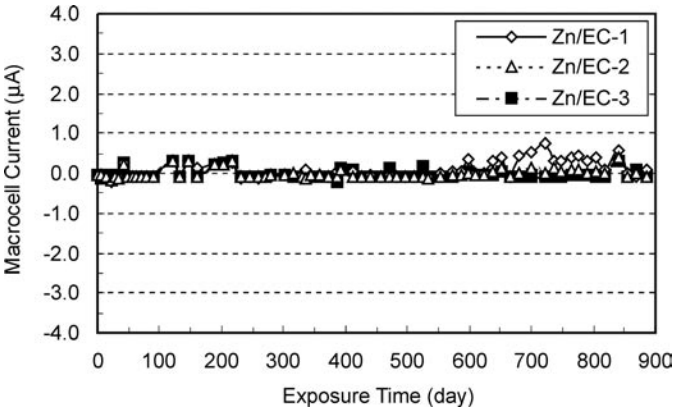

Fig. 7: Macrocell current of the concrete blocks with Zn/EC bars in three different coating conditions

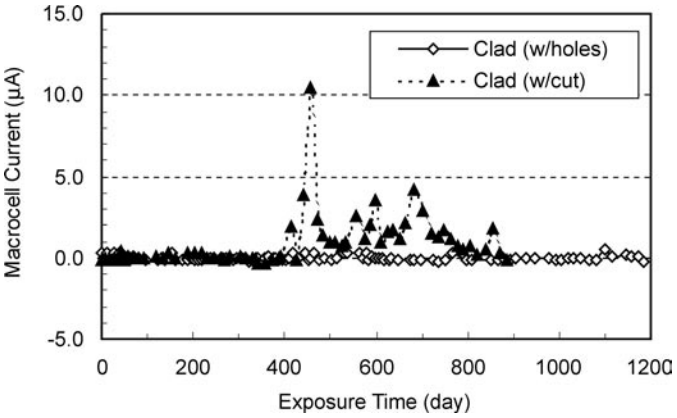

Fig. 8: Macrocell currents of the concrete blocks with the 316L-clad bars with either holes or a cut introduced through the cladding

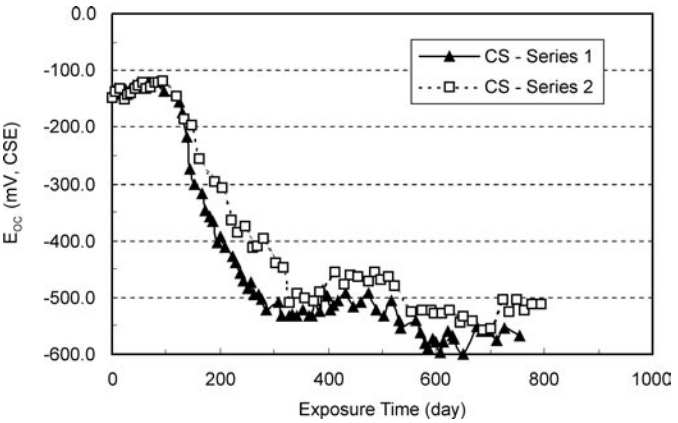

Fig. 9: Open-circuit potentials of the carbon steel bars in both series of concrete blocks

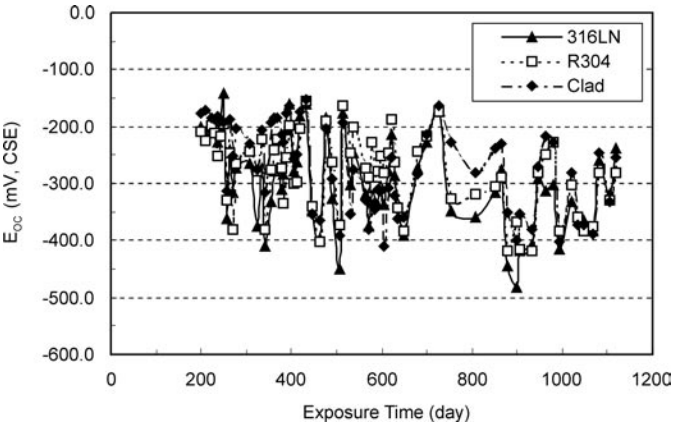

Fig. 10: Open-circuit potentials of the 316LN, R304, and 316L-clad bars

In contrast, there were no significant macrocell currents in the blocks with the Zn/EC bars until after 76 to 79 weekly cycles of salt exposure when the Zn/EC-1 bars began to indicate some activity (Fig. 7). There was no apparent activity, even after 899 days of exposure, on the Zn/EC-2 bars or the Zn/EC-3 bars.

The 316L-clad bars with three holes drilled through the cladding had no significant macrocell current, even after 1186 days of exposure (Fig. 8). In contrast, the 316L-clad bars with a cut intentionally introduced through the cladding began to show measurable positive macrocell current at 392 days, however, the maximum macrocell current exhibited was only 10.5 µA on Day 456, which is comparatively less than the currents observed on the CS, the unpickled 2101 LDX, and the unpickled microcomposite steel bars. Regardless, this likely indicates that the exposed CS core had begun to corrode.

Open-circuit potentials

Another parameter monitored weekly was the open-circuit potentials of each bar that was used at both the top and the bottom of the concrete block. In general, when the potentials of CS bars in concrete become more negative than –350 mV (CSE), the probability that the bars are corroding is considered to be very high.

According to Fig. 9, which shows the potentials of the CS bars in both series of concrete blocks as a function of their exposure times, their potentials were relatively stable for the first 92 to 95 days, ranging between –118 and –138 mV (CSE). This was then followed by a period of 217 to 225 days in which the potential became precipitously more negative for both groups of CS bars—shifting by an average of –1.7 to –1.8 mV/day. Thereafter, the potentials of these bars eventually became as negative as –556 to –600 mV. Interestingly, the turning point of the potentials at 92 to 95 days coincided well with the 90 to 95 days required for the weekly macrocell currents of these bars to show rapid increases—both signaling the beginning of corrosion activity.

In contrast, the potentials of the 316LN, the R304, and the 316L-clad bars exhibited an almost common behavior: a relatively slow but steady trend toward electronegativity—

at a rate of approximately –0.11 mV/day—with some large potential fluctuations from week to week (Fig. 10). Further, the potentials of these bars were almost indistinguishable, even after 1100 days—an indication that the R304 and the 316L-clad bars behaved similarly to the 316LN.

Meanwhile, the potentials of the unpickled 2101 LDX and microcomposite bars behaved almost like that of the CS bars—abruptly shifting electronegatively after some initial period of stability—but longer than that for the CS bars: 147 and 247 days for the unpickled 2101 LDX and microcomposite steel, respectively (Fig. 11). Again, these two turning points in their potentials were in good agreement with the observed times at which these two bars started to exhibit significant increases in their macrocell currents—147 and 245 days for the unpickled 2101 LDX and microcomposite steel, respectively.

In contrast, as Fig. 12 shows, the potentials of all three groups of Zn/EC bars were considerably more stable—shifting only –60, –63, and –22 mV in approximately 900 days for the Zn/EC-1, Zn/EC-2, and Zn/EC-3 bars, respectively. In all cases, the initial potentials of these three groups of Zn/EC bars—ranging between –305 and –360 mV—reflected the influence of the zinc coating, which is more anodic or reactive than the black steel substrate. Beyond this, it is difficult to elucidate the meaning of the stability of these potentials.

The potentials of the 316L-clad bars with small holes drilled through their cladding were similar to those of the 316L-clad bars without damage. However, when the cladding defect was a large cut, the potentials behaved similar to those of the CS, the 2101 LDX, and the micro-composite bars. After an initial period (approximately 392 days) of stable potentials, which fluctuated around –180 mV, the potential shifted by as much as –155 mV in 55 days, or –2.8 mV/day—more than the shifts of –1.7 to –1.8 mV/day observed on the CS bars. The potentials then remained practically stable for a period of almost 300 days before, interestingly, reversing or shifting cathodically. At about 800 days, the potentials had returned to almost the same levels as at the beginning of the salting of the concrete blocks containing these 316L-clad bars.

CHLORIDE ION CONCENTRATIONS IN THE TEST BLOCKS

As shown in the preceding sections, the macrocell current and open-circuit potential of a metallic reinforcing bar reflects its corrosion state. Therefore, by weekly monitoring these two simple electrochemical parameters, as the different bars were being regularly exposed to salt, the time-to-corrosion of these bars can be effectively pinpointed. Table 4 lists the time-to-corrosion of the different bars. Although this time parameter is useful for comparing the bars, a more useful indicator would be the amount of chloride ions that each type of bar was able to

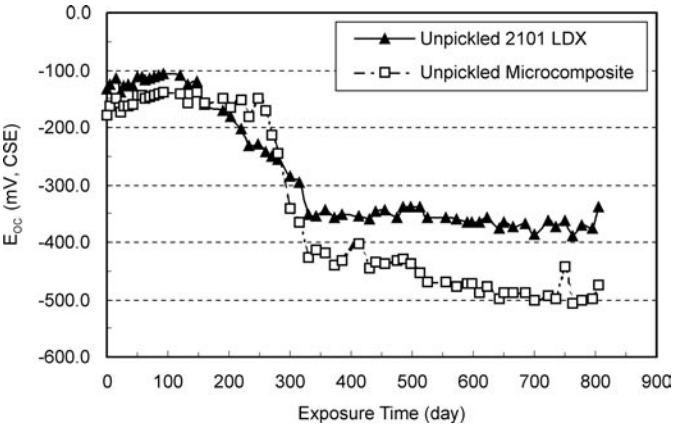

Fig. 11: Open-circuit potentials of the unpickled 2101 LDX and microcomposite bars

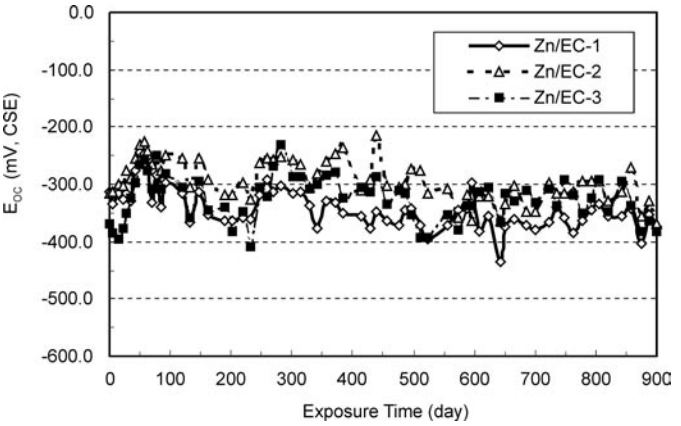

Fig. 12: Open-circuit potentials of the Zn/EC bars with three different coating conditions

tolerate in the concrete—its chloride corrosion threshold.

To equate the estimated time-to-corrosion of each bar to its chloride corrosion threshold, the mean chloride concentrations in the concrete blocks at different depths were determined by analysis of the ground concrete samples extracted from 16 randomly selected test concrete blocks, after several different exposure times. From the best-fit curves for these several chloride ion distributions, the mean concentration of the chloride ions in the test blocks at the depth of the top-mat bars—33 mm (1.3 in.)—as a function of exposure time was derived. This function, in turn, provided estimates of the chloride corrosion thresholds of the various bars, listed in Table 4.

CURRENTS AND POTENTIALS AGREE

Examination of all electrochemical data collected would indicate that both the macrocell current and the potential, in relation to exposure time, indicate when corrosion has begun on a particular type of bar. As clearly demonstrated in Fig. 2, the onset of corrosion in the

TABLE 4:
ESTIMATED RELATIVE TIMES-TO-CORROSION AND CHLORIDE THRESHOLD CONCENTRATIONS FOR THE DIFFERENT BARS

Bar	Time-to-corrosion, day	Chloride threshold, ppm	Threshold ratio
Carbon steel	90 to 95	460 to 580	1.0
2101 LDX	144 to 147	1520 to 1560	2.6 to 3.4
Microcomposite	244 to 247	2700 to 2730	4.7 to 6.0
316L-clad with cut	392 to 413	3770 to 3890	6.5 to 8.5
Zn/EC-1	532 to 554	4460 to 4550	7.7 to 10.0
Zn/EC-2	>899	>5640	>9.8 to 12.4
Zn/EC-3	>899	>5640	>9.8 to 12.4
316L-clad with holes	>1299	>6470	>11.2 to 14.2
316L-clad	>1299	>6470	>11.2 to 14.2
R304	>1299	>6470	>11.2 to 14.2
316 LN	>1299	>6470	>11.2 to 14.2

CS bars was clearly characterized by a rise in the positive macrocell current in the concrete blocks. Concurrently, the potentials of these metallic bars showed relatively rapid shifts toward electronegativity (Fig. 9 and 12). In contrast, the other bars, which were relatively more passive or corrosion resistant, exhibited no significant macrocell currents and considerably more stable potentials for much longer exposure times. Based on the exposure time at which each type of bars began to show significant changes in these two simple parameters, we estimated the time-to-corrosion of the different types of bars.

Table 4 lists the estimated relative times-to-corrosion and chloride corrosion thresholds of the different bars in increasing order, including the 316L-clad and Zn/EC bars with intentionally introduced damages. It must be emphasized that the testing of the last six groups of bars, those that have not corroded yet, is still in progress. Therefore, the relative rankings of these six groups are yet to be determined. It would not surprising if the time-to-corrosion for the Zn/EC-2 and Zn/EC-3 bars is shorter than those of the R304, the 316L-clad, and the 316LN bars—because the latter bars are not as susceptible to abrasion damage as the former bars and have already been tested for almost 400 days longer.

This investigation estimated that the conventional CS bars were able to withstand from 460 to 580 ppm of chloride in the concrete blocks, or 0.046 to 0.058% by weight of concrete, before corroding (Table 4). Previous investigators have reported threshold levels of 330 to 670 ppm.[7,8] Considering the differences in the manners with which the previous and the present investigators arrived at these threshold values, these values can be considered to be in good agreement.

Based on their estimated times-to-corrosion, the 2101 LDX and microcomposite steel bars appear capable of resisting 2.6 to 3.4 times and 4.7 to 6.0 times, respectively, more chloride ions than the CS bars. Although not within the initial scope of this ongoing investigation, we pickled a limited number of the 2101 LDX and microcomposite bars received from the suppliers with an aqueous solution of nitric and hydrofluoric acids at 60 °C (140 °F). Subsequent testing of these pickled samples—in solutions of various chloride concentrations and pHs, using potentiodynamic, potentiostatic polarization methods, and the like—has revealed that pickling would improve the chloride corrosion thresholds of both 2101 LDX and the microcomposite steel bars by several times.[9]

In the present investigation, because the R340, the 316L-clad, and the 316LN bars were still passive after 1299 days of weekly salt exposure, the threshold levels of these bars would be higher than 6470 ppm, or at least 11.2 to 14.2 times that of CS. This is in agreement with earlier reports regarding specific stainless steels (such as 304, 316, and N33) that there were no significant differences in the resistances of these metallic bars to chloride ions and the chloride threshold levels of these bars ranged from more than 10 to 24 times that of CS.[2,4,5,10]

The effect of cladding damage or defect on the corrosion resistance of 316L-clad bars is an interesting issue. As indicated in the earlier discussion, when the defect or damage was a cut of 25-mm-long (1.0 in.) and 1-mm-wide (0.04 in.) in each of the top 316L-clad bars, these bars began to show positive mean macrocell current between them and the bottom 316L-clad bars and an abrupt shift toward electronegativity in their mean open-circuit potentials at approximately 392 days. This signaled that corrosion was initiated on some of these 316L-clad bars with cuts.

For visual confirmation, block CB (w/cut) –1 was autopsied to expose the two top 316L-clad bars. This revealed that bar 1A had no sign of corrosion at the cut, while bar 1B had two round corrosion areas—one at each end of the cut. Further examination of bar 1B revealed no further damage to the bar, and that the corrosion in both

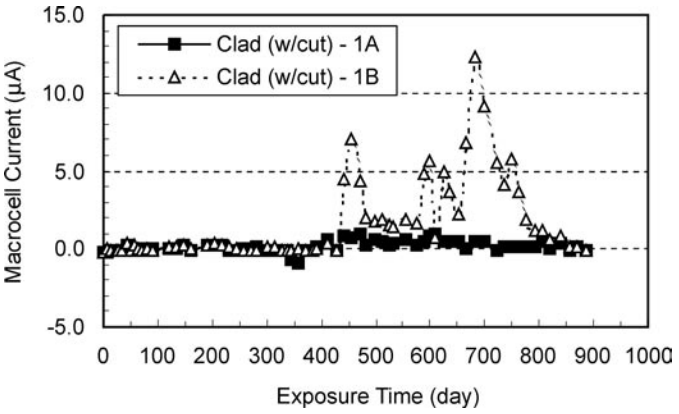

Fig. 13: The macrocell currents flowing between 316L-clad bars with cuts 1A and 1B and their respective accompanying bottom clad bars

Fig. 14: One of the holes (marked area in the center) drilled through the cladding of a 316L-clad bar. Notice the absence of any sign of corrosion around the hole, even though it was apparently not filled with cement paste

areas may have subsided. The macrocell currents of these individual bars strongly reflect the apparent absence of corrosion on bar 1A, and the initiation and then probable subsidence of corrosion on bar 1B (Fig. 13). As shown, there was no significant macrocell current for bar 1A, even though it had a cut similar to that in bar 1B, which exhibited macrocell current from approximately day 400. The relatively smaller magnitude of the macrocell current in bar 1B, when compared to those of the CS, 2101 LDX, and microcomposite bars, and its continuous decreasing trend in the last 100 days, may be an indication that the corrosion did not continue to propagate, or at least not at a fast rate. Future plans include slicing bar 1B at the vicinity of the cut to allow for close examination of the cladding/core interface at the two corrosion areas.

The remaining two similar bars (2A and 2B) also exhibited significant, but similarly small, macrocell currents—with one bar starting at approximately 392 days. This means that three-quarters of the 316L-clad bars with a cut have begun to corrode.

In contrast, the absence of macrocell current for the entire 1299 days of testing of the 316L-clad bars with holes drilled through the cladding (Fig. 8) suggested no corrosion yet on these bars. Similar autopsy of a concrete block with two of these bars confirmed no sign of corrosion around each of the holes (Fig. 14). These results certainly point toward a possible influence of cladding defect size on loss of protection for the CS core. The cuts introduced on some of the 316L-clad bars in this investigation were probably unrealistic. Although it is expected that the stainless steel cladding would be very resistant to damage by impact, abrasion, or penetration, it is conceivable that cladding "breaks" can occur if sections of bars with insufficient cladding are bent.

The results on the 316L-clad bars with the cuts raise an interesting question: Why didn't the area of CS core exposed directly to the cement paste (and, therefore, chloride ions), through the cut in the cladding, behave like a conventional CS bar, instead of having an effective chloride threshold that is 6.5 to 8.5 times higher (see Table 4)?

The issue regarding the effect of defects on the protection provided by the composite coating system on the Zn/EC bars is similarly interesting. As their macrocell currents indicate, the defect-free Zn/EC-3 bars remained passive—even after almost 900 days of the weekly severe salt exposure. Those with a cut through the epoxy coating only (Zn/EC-2) performed equally well. Even the appearance of corrosion activity on the Zn/EC-1 bars, as shown in Fig. 7, after 532 to 554 days, is encouraging—especially when the magnitude of the observed macrocell current is taken into consideration. It must be emphasized, though, that the fine 25 mm cuts introduced through the coatings are likely not representative of the types of coating damage that conventional epoxy coating bars are often subjected to at construction sites, which can be relatively wider and widespread. Nevertheless, the data presented appeared to indicate that the provision of the extra layer of Zn may be serving its intended purpose.

Similar autopsy of three different concrete blocks, one each for Zn/EC-1, -2, and -3 bars, confirmed that: 1) there was no corrosion yet on any one of the two Zn/EC-2 or -3 bars exposed; and 2) not surprisingly, one of the Zn/EC-1 bars, the 1A, had no sign of corrosion yet around the cut, while the other bar in the same block, the 1B bar, had four small corrosion areas—all within 22 mm (0.9 in) of the cut through both the Zn and the epoxy coating (Fig. 15). As in the case of the two exposed 316L-clad bars with the cut, this is supported by the changes in the macrocell

Fig. 15: The Zn/EC-1-1B bar recovered from a concrete block. Notice the four corrosion areas that ranged from 2 to 5 mm (0.08 to 0.20 in.) across and at 0 to 22 mm (0 to 0.9 in.) from the cut in the composite coating system

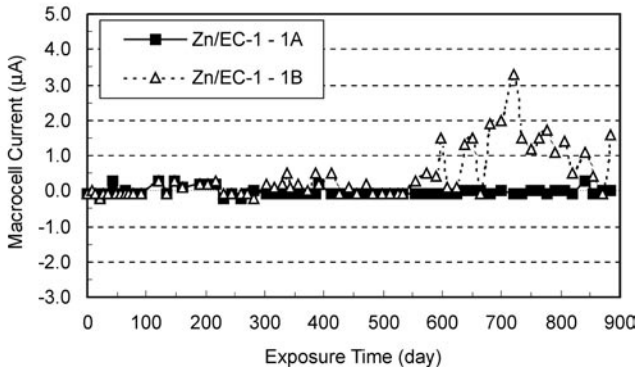

Fig. 16: The macrocell currents flowing between Zn/EC-1-1A and –1B bars and their respective accompanying bottom Zn/EC bars

currents—as a function of salt exposure time—for these two individual bars (Fig. 16).

BARS SHOW DURABILITY POTENTIAL

In this more than 3 year testing time frame, the unconventionally made R304 bars appear to possess the same resistance to high concentrations of chloride in concrete as the 316LN bars. The defect-free 316L-clad bars have also shown excellent corrosion resistance—indicating that the stainless steel cladding is providing the intended protection for the CS core. Depending on their size, defects in the cladding may negate this protection somewhat. There is evidence that corrosion on the core caused by cladding defect, however, may be slow compared to corrosion of unclad CS bars. Comparatively, the unpickled 2101 LDX and microcomposite bars appeared to have corrosion resistances better than the CS bars, but worse than the 316LN, the R304, and the defect-free 316L-clad bars. The addition of an arc-sprayed Zn coating, between the mild steel bars and the epoxy coating, appeared to improve the durability of current ECR in salt-contaminated concrete. Regretfully, no plain ECR were included for control.

Last, it could be risky to use a combination of a more expensive corrosion-resistant bar in the top-mat reinforcement of a concrete bridge deck and the cheaper but corrosion-susceptible CS bars in the bottom mat. Depending on the permeability of the concrete, sufficient chloride ions could reach the bottom CS bars during the life of a structure to cause them to corrode before the more corrosion-resistant top bars—in which case, the consequential necessary repairs to the structure would be extremely more difficult and costly.

References

1. Hurley, M. F.; Scully, J. R.; and Clemeña, G. G., "Selected Issues in Corrosion Resistance of Stainless Steel Clad Rebar," *Corrosion 2001*, National Association of Corrosion Engineers-International, Houston, TX, 2001.

2. Zoob, A. B.; LeClaire, P. J.; and Pfeifer, D. W.; "Corrosion Tests on Reinforced Concrete With Solid Stainless Steel Reinforcing Bars for Joslyn Stainless Steels," Wiss, Janney, Elstner, Inc., Northbrook, IL, 1985.

3. McDonald, D. B.; Pfeifer, D. W.; and Blake, G. T., "The Corrosion Performance of Inorganic-, Ceramic-, and Metallic-Clad Reinforcing Bars and Solid Metallic Reinforcing Bars in Accelerated Screening Tests," *Report No.* FHWA-RD-96-085, Federal Highway Administration, Washington, DC, 1996.

4. Gu, P.; Elliot, S.; Beaudoin, J. J.; and Arsenault, B., "Corrosion Resistance of Stainless Steel in Chloride Contaminated Concrete," *Cement and Concrete Research*, V. 26, No. 8, 1996, pp. 1151-1156.

5. McDonald, D. B.; Pfeifer, D. W.; and Sherman, M. R., "Corrosion Evaluation of Epoxy-Coated, Metallic-Clad and Solid Metallic Reinforcing Bars in Concrete," *Report No.* FHWA-RD-98-153, Federal Highway Administration, Washington, DC, 1998.

6. Broomfield, J. P.; Rodriquez, J.; Ortega, L. M.; and Garcia, A. M., "Corrosion Rate Measurement and Life Prediction for Reinforced Concrete Structures," Proceedings of the Structural Faults and Repairs – 1993, University of Edinburg, Scotland, V. 2, 1993, pp. 155-164.

7. Lewis, D. A., "Some Aspects of the Corrosion of Steel in Concrete," *Proceedings of the First International Congress on Metallic Corrosion,* London, 1962, pp. 547-555.

8. Pettersson, K., "Chloride Threshold Value and the Corrosion Rate in Reinforced Concrete," *Cement and Concrete Research*, V. 24, 1994, pp. 461-470.

9. Scully, J. R., and Clemeña, G. G., "Work Plan: Investigation of the Corrosion Propagation Characteristics of New Metallic Reinforcing Bars," Virginia Transportation Research Council, Charlottesville, VA, 2002.

10. Nurnberger, U.; Beul, W.; and Onuseit, G., "Corrosion Behavior of Welded Stainless Reinforcing Steel in Concrete," *Otto Graf Journal*, V. 4, 1993, pp. 225-259.

Selected for reader interest by the editors after independent expert evaluation and recommendation.

Gerardo G. Clemeña is a Research Scientist with the Virginia Transportation Research Council. He received his PhD in analytical chemistry and MSc in physical chemistry from the University of Virginia. His research interests include mitigation of steel corrosion in existing concrete bridges with electrochemical treatment, prevention of corrosion in new concrete bridges with the use of corrosion-resistant bars, applications of nondestructive evaluation techniques, and structural integrity monitoring.

Yash Paul Virmani is a Program Manager with the Office of Infrastructure R&D of the Federal Highway Administration. He received his PhD in physical chemistry from the University of Bombay and MSc in physical chemistry from the University of Rajasthan, India, in 1958. He has been responsible for research on corrosion in reinforced and prestressed concrete and cable-stay bridges for the last 20 years. Virmani is also responsible for development of cost-effective corrosion protection systems for new construction and rehabilitation of existing salt-contaminated concrete bridges. He is presently the program coordinator for the NACE International symposia and technical information exchanges in the area of infrastructure. Virmani is currently conducting a congressionally mandated study of cost of corrosion and preventive strategies.